Scientific Research Publishing

Open Journal of Energy Efficiency, 2022, 11, 55-70
https://www.scirp.org/journal/ojee
ISSN Online: 2169-2645
ISSN Print: 2169-2637

A New Control Approach of a Three-Phase Inverter Two Levels

François Yonga[1], Colince Welba[2], Theodore Louossi[1], Noël Djongyang[1*]

[1]Department of Renewable Energies, National Higher Polytechnic School of Maroua, University of Maroua, Maroua, Cameroon
[2]Department of Fundamental Sciences, National Advanced School of Mines and Petroleum Industries, University of Maroua, Maroua, Cameroon
Email: yongafrancois@gmail.com, welbacolince@yahoo.fr, *noeldjongyang@gmail.com

How to cite this paper: Yonga, F., Welba, C., Louossi, T. and Djongyang, N. (2022) A New Control Approach of a Three-Phase Inverter Two Levels. *Open Journal of Energy Efficiency*, **11**, 55-70.
https://doi.org/10.4236/ojee.2022.113005

Received: January 27, 2022
Accepted: September 4, 2022
Published: September 7, 2022

Abstract

In this paper, we present the study, modelling and simulation of the duty cycle modulation (DCM) based on SVPWM control technique using Matlab/Simulink software. It is one of the most advanced control techniques of space vector modulation (SVM), which can be used for controlling static converters or for controlling electrical machines to achieve better dynamic performance. DCSVM is a control technique that generates control signals for the two-level voltage converter as well as for the intermediate times. The main advantage of this control technique is the reduction of the number of calculations, especially for the trigonometric functions and the generation of the reference voltage. In order to reduce the computational effort, we have designed a DCSVM controller that is able to faithfully reproduce the same vectors and output quantities as a classical SVM. In order to test the functionality and validity of the DCSVM control, we have developed different simulations that result in a total harmonic distortion (THD) of the voltage and current of 41.19% and 15.19% respectively with fundamental values of 61.51 V for the voltage and 2.80 A for the current; in contrast to the SVM which gives 47.27 V for the voltage and 2.01 A for the current with THDs of 77.16% for the voltage and 16.00% for the current. This results in an improvement in the distortion rate of around 25.5%. The results obtained are very satisfactory. The DCSVM is a real competitor to the SVM and its various variants.

Keywords

Inverter, SVM (Space Vector Modulation), DCSVM (Duty Cycle Space Vector Modulation), Harmonic, THD (Total Harmonic Distorsion)

1. Introduction

The increasing use of power electronic components in electrical networks has an impact on power quality [1]. Depending on the type of load and the user's needs, the signal provided by solar inverters must be of very high quality [1] [2]. In general, there is a close relationship among efficiency, cost and complexity. This relationship is evident when analysing the main parameters obtained in each design [3]. Parameters include harmonic distortion rate, current leakage and efficiency. In an on-grid photovoltaic (PV) system, proper inverter control is necessary to achieve moderate power loss, low total harmonic distortion (THD), safety and reliability of the grid [4] [5]. Different types of control mechanisms, including linear mechanisms (proportional-integral (PI), proportional-resonant (PR), repetitive, dead time control, etc.) and non-linear techniques (sliding mode control (SMC), space vector modulation (SVM), prediction, etc.) [3] [6] [7] [8] are available in the literature. Modulation theory has a major research area in signal transmission, signal processing, Analog-to-Digital Conversion (ADC), Digital-to-Analog Conversion (DAC) and control of power electronic converters and continues to attract considerable attention and interest [9] [10] [11]. The switching modulation which includes Sigma-Delta Modulation (SDM), Pulse Width Modulation (PWM) and Duty-Cycle Modulation (DCM) is a type of modulation widely used for industrial applications [11]. Other recent works that present a signal modulation technique with attracting features have been reported [12] [13]. Among them, the duty cycle modulation (DCM) method addressed in [14] has the particularity of producing fewer harmonics [15]. Another peculiarity of the DCM is its modulation frequency which is a function of the amplitudes of the modulating signal. The work of [16] presents the DCM as an efficient tool in the modulation of transmission signals via high quality results. However, the work in [12] presents an application of the DCM in the control of a single-phase inverter. The results presented show that it is necessary to use a transformer in order to have a fundamental signal with an amplitude higher than its reference. This control strategy, initiated since 2005 [14] for industrial instrumentation purposes, has led to other scientific work [17] [18] which has proven its reliability and efficiency. Given that the theoretical study, based on virtual simulations, has already been successfully carried out in recent works, on a new topology of IDCM (inverters with duty cyclic modulation) [2]. This scientific paper deals with a new control approach applied to a three-phase inverter based on controller with duty cycle. This strategy is called duty cycle space vector modulation (DCSVM). In this paper, we present the modeling and simulation of new control technique, as alternative to the classical SVPWM, implemented with duty cycle regulator using Matlab/Simulink software, in order to use it for the command or control of static converters. In order to test the feasibility of DCSVM controllers, simulations have been carried out, the results obtained agree perfectly with those obtained with a conventional SVPWM controller. The remaining part of this paper is organized as follows: The inverter system

configuration used for the study is presented in Section 2. Section 3 is devoted to a brief description of different control techniques and analysis of proposed DCSVM strategy. Section 4 includes simulation results and discussion. Finally, we end with a conclusion where we highlight the value of this best-performing ordering strategy is giving in Section 5.

2. Presentation of the Studied System

Figure 1 shows the configuration of a block diagram of the solar PV system based inverter electric power supply system as consisting of an interconnection of solar PV array, a backup battery with the maximum power point tracker (MPPT) buck/boost converter, an inverter, a filter, a load and a control system that uses specified control algorithms.

In this paper, we will axe our work on the command of an inverter with a DCSVM as an alternative the conventional SVM control. The solar array can be assumed to deliver power to the load through an "optimized inverter". The optimization of inverter involves conditioning the unregulated solar array dc supply (at its maximum power operating point for given sun radiation) to predetermined voltage/current and frequency values required by both the load and the back-up battery on charge [14] [17] [18] [19]. In Figure 2, we show the structure of the three-phase two-level inverter to be controlled.

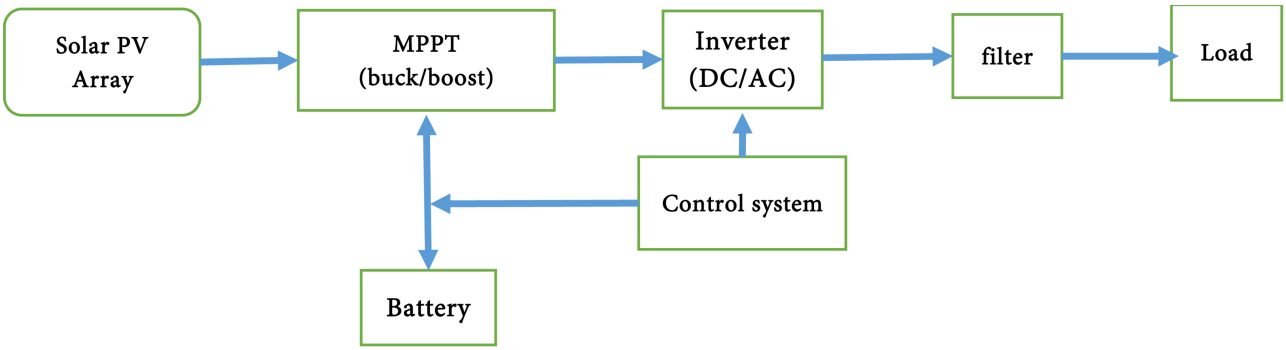

Figure 1. The configuration of a block diagram of the solar PV system.

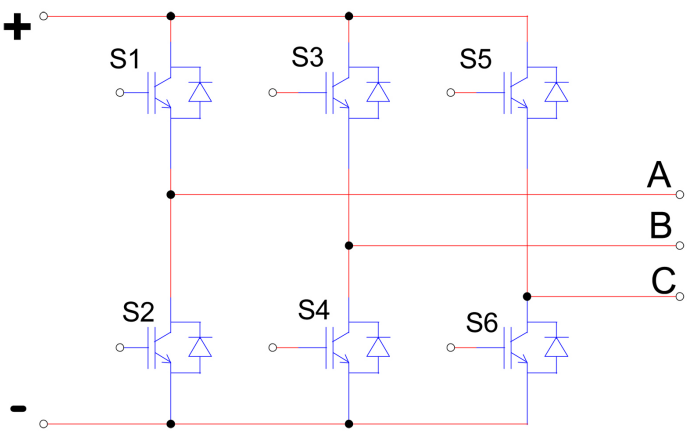

Figure 2. Structure of the three-phase inverter controlled.

In the following, we will apply our control strategy to the structure shown in **Figure 2** and discuss the results obtained from the simulation.

3. Theory of Control Techniques

3.1. Space Vector Modulation

The space vector modulation technique (SVM ou SVPWM: Space Vector Pulse Width Modulation) is a variant of the pulse width modulation control which is based on the vector representation of the voltages in the complex plane [4] [20] [21] [22]. SVM control technology is used for conventional single-phase and three-phase inverters [12] [23]. It applies well to neutral point voltage balancing problems, making it flexible and also reducing switching losses in switches [12] [14] [24] [25]. From the three-phase inverter in **Figure 2**, we will measure the current and voltage in one phase of the inverter. Various PWM techniques have been developed for industrial applications. The most commonly used PWM schemes for three-phase voltage inverters are Space Vector PWM (SVPWM) [5] [6] [20] [22]. The principle of vector modeling consists in reconstructing the voltage vector from eight voltage vectors [5]. Each of these vectors corresponds to a combination of the state of the switches of the three-phase voltage inverter. It does not rely on separate modulation calculations by each inverter arm [20] [22]. The Construction of the output vectors of the three-phase inverter and the different states of the inverter are given in [5] [22]. This technique follows the following principles:

A reference vector is calculated globally and approximated over a modulation period T_s;

All half-bridge switches have an identical state at the centers and at the ends of the period. A combinatorial analysis of all the possible states of the switches makes it possible to calculate the voltage vector (v_α, v_β), according to the System (1). [6] [20]

$$\begin{bmatrix} v_\alpha \\ v_\beta \end{bmatrix} = \sqrt{\frac{2}{3}} \begin{pmatrix} 1 & -\frac{1}{2} & -\frac{1}{2} \\ 0 & \frac{\sqrt{3}}{2} & -\frac{\sqrt{3}}{2} \end{pmatrix} \begin{bmatrix} v_{AN} \\ v_{BN} \\ v_{CN} \end{bmatrix} \tag{1}$$

The vector v_α is approximated over the modulation period, by the generation of an average vector developed by the application of the vectors. It consists in considering the three-phase system globally, and in applying a Concordia transformation to it to be brought back to the plane (v_α, v_β) [5] [20] [22]. The sampling time can then be represented as a single vector in this plane [6]. The major drawback of SVPWM is the enormous computational time required for its implementation due to the trigonometric functions used to determine the times T_k and T_{k+1} [20]. When PWM is used to control solid state switches, a relatively high frequency carrier is required to reduce current and voltage ripple and THD [8]. This increase in frequency leads to switching losses [12] [19] on the one hand, and to thermal stress at the switches on the other hand [8] [20], hence the

interest of improving it by using the duty cycle regulator. Recent literature [12] [13] [14] [15] presents the duty cycle modulation (DCM) method as a signal modulation technique with interesting characteristics and the particularity of producing fewer harmonics.

3.2. Duty-Cycle Modulation (DCM)

In the past, inverters were controlled only using PWM (pulse width modulation) based drivers, but nowadays it is also done from drivers based on the DCM [2]. The DCM is a modulation in which an input signal x is transformed into a train of switching wave where duty cycle and period of the modulated signal vary simultaneously according to control signal [14] [16] [26]. Initially invented and patented by Biard *et al.* in 1962, the realization of classical DCM circuit requires at least two integrated circuits and seven passive elements [23] [27]. Initially proposed for instrumentation problems, they are today used in many sectors such as ADC [14] [28], DAC [17], control of electronic power converter [13] [29], digital signal transmission [26], power quality [30] [31] [32] and optical transmission [7]. **Figure 3(a)** shows the basic electronic circuitry of the DCM while its mathematical model is described by Equation (2).

This structure, although functional and allowing low-frequency operation, has some drawbacks, among which: The non-linearity of the function linking the

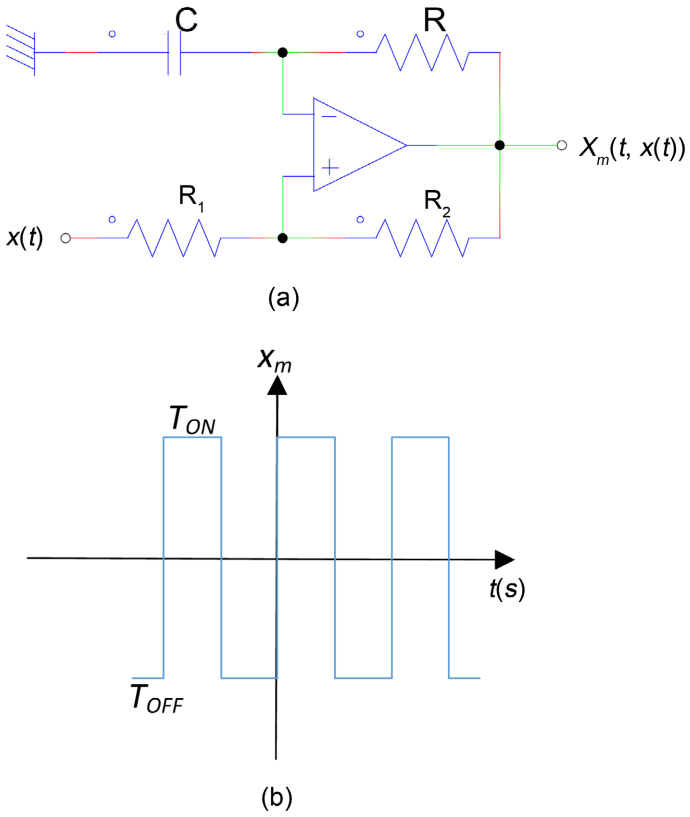

Figure 3. Duty cycle modulation (a) Electronic circuit of duty cycle modulator; (b) Example of duty cycle modulation output signal [3] [26].

duty-cycle to the control signal and the dependence of the duty-cycle on the values of the passive components [11].

$$\begin{cases} u(t)^{+} = \alpha_1 x_m\left(t, x(t)\right) + (1-\alpha_1)x(t) \quad \text{with } \alpha_1 = \dfrac{R_1}{R_1+R_2} \\ \varepsilon(t) = u(t)^{+} - u(t)^{4} = u(t)^{+} - u_C(t) \\ x_m\left(t, x(t)\right) = \begin{cases} +E, \text{ if } \varepsilon(t) \geq 0 \\ -E, \text{ otherwise} \end{cases} \\ \dfrac{\mathrm{d}u_C(t)}{\mathrm{d}t} = -\dfrac{1}{RC}\left(u_C(t) + x_m\left(t, x(t)\right)\right) \end{cases} \tag{2}$$

The high level time T_{on}, the carrier period T_m, the duty cycle R_m and the low level time T_{off} give as shown in Equation (3) [3].

$$\begin{cases} T_{on}\left(x(t), \alpha\right) = RC\ln\left(\dfrac{(1-\alpha)x(t) - (1+\alpha)E}{(1-\alpha)x(t) + (\alpha+1)E}\right) \\ T_m\left(x(t), \alpha\right) = RC\ln\left(\dfrac{\left((1-\alpha)x(t)\right)^2 - \left((1+\alpha)E\right)^2}{\left((1-\alpha)x(t)\right)^2 + \left((\alpha+1)E\right)^2}\right) \\ R_m\left(x(t), \alpha\right) = \dfrac{T_{on}\left(x(t), \alpha\right)}{T_m\left(x(t), \alpha\right)} \\ T_{off}\left(x(t), \alpha\right) = T_m\left(x(t), \alpha\right)\left(1 - R_m\left(x(t), \alpha\right)\right) \end{cases} \tag{3}$$

This modulator has the advantage of being simpler than a PWM modulator. Its period T_m and duty cycle α are defined by [29]:

$$\begin{cases} T_m\left(x(t), \alpha\right) = RC\ln\left(\dfrac{\left((1-\alpha)x(t)\right)^2 - \left((1+\alpha)E\right)^2}{\left((1-\alpha)x(t)\right)^2 + \left((\alpha+1)E\right)^2}\right) \\ \alpha = \ln\left(\dfrac{\left((1-\alpha)x(t)\right)^2 - \left((1+\alpha)E\right)^2}{\left((1-\alpha)x(t)\right)^2 + \left((\alpha+1)E\right)^2}\right) \\ \alpha_1 = \dfrac{R_1}{R_1+R_2} \text{ and } \alpha_2 = \dfrac{R_2}{R_1+R_2} \end{cases} \tag{4}$$

Its minimum or central period and duty cycle (for $x(t) = 0\, xt{=}0$) are given by:

$$\begin{cases} T_m(0) = 2RC\ln\left(1 + 2\dfrac{R_1}{R_2}\right) \\ \alpha = \dfrac{1}{2} \end{cases} \tag{5}$$

The DCM method discussed has the particularity of producing harmonics. Another particularity of DCM is its modulation frequency which is a function of the amplitude of the modulating signal. The major drawback is the imperative need to use a low-pass filter to eliminate the high frequencies. Subsequently, a new, simpler and better control strategy is proposed to combine the advantages

of SVM and DCM.

3.3. New Proposed Command

The principle of the DCSVM control is based on the advantages of the DCM control and the classical SVM control. The implementation of the DCSVM strategy is carried out in the following steps:

Step 1: Determination of reference voltage (v_α , v_β)

The generation of vectors in the Concordia landmark (d, q) from the three-phase signals (v_{AN} , v_{BN} , v_{CN}) is given by the Relation (6):

$$\begin{cases} v_d = \frac{2}{3}\left(v_{AN} - \frac{v_{BN}}{2} - \frac{v_{CN}}{2} \right) \\ v_q = \frac{\sqrt{3}}{3}\left(v_{BN} - v_{CN} \right) \end{cases} \tag{6}$$

$$\begin{bmatrix} v_d \\ v_q \end{bmatrix} = \frac{1}{3}\begin{pmatrix} 1 & -1 & -1 \\ 0 & \sqrt{3} & -\sqrt{3} \end{pmatrix}\begin{bmatrix} v_{AN} \\ v_{BN} \\ v_{CN} \end{bmatrix} \tag{7}$$

Step 2: Cartesian to polar transformation

The system of equations gives in Equation (8) transforms corresponding elements of the two-dimensional Cartesian coordinate arrays d and q into polar coordinates (ρ , θ).

$$\begin{cases} \rho = \sqrt{v_d^2 + v_q^2} \\ \theta = \tan^{-1}\left(\frac{v_q}{v_d} \right) \end{cases} \tag{8}$$

Step 3: Generation of control signals and intermediate times

The Simulink model is used to determine the control signals for switches T_{ag}, T_{bg} and T_{cg}, and the intermediate times T_1, T_2 and T_0.

Furthermore, assuming that the reference voltage vector V_{ref} is synthesized from the two basic vectors, the operating time of two basic vectors can be calculated according to the volt-second equilibrium principle [29].

$$\begin{cases} T_1 = \sqrt{3}\left(\frac{V_{ref}}{V_{dc}} T_S \right) \sin\left(\theta - \frac{(k-1)\pi}{3} \right) \\ T_2 = \sqrt{3}\left(\frac{V_{ref}}{V_{dc}} T_S \right) \sin\left(\frac{k\pi}{3} - \theta \right) \\ T_0 = T_S - T_1 - T_2 \end{cases} \tag{9}$$

With: T_1 and T_2: times allocated to vectors $\boldsymbol{V}_1$ and $\boldsymbol{V}_2$, T_0: time shared between the two null vectors $\boldsymbol{V}_7$ and $\boldsymbol{V}_9$, and T_S: half-carrier time period.

After determining the times T_1, T_2 and T_0, the time of the closing all keys to the rack at work is determined. In each sector the switching time of each key is different and is expressed in (10):

$$\begin{cases} \text{for } \theta = \left]0, \frac{\pi}{3}\right]; \text{we get} : S = 1 \\ \text{for } \theta = \left]\frac{\pi}{3}, \frac{2\pi}{3}\right]; \text{we get} : S = 2 \\ \text{for } \theta = \left]\frac{2\pi}{3}, \pi\right]; \text{we get} : S = 3 \\ \text{for } \theta = \left]\pi, \frac{4\pi}{3}\right]; \text{we get} : S = 4 \\ \text{for } \theta = \left]\frac{4\pi}{3}, \frac{5\pi}{3}\right]; \text{we get} : S = 5 \\ \text{for } \theta = \left]\frac{5\pi}{3}, 2\pi\right]; \text{we get} : S = 6 \end{cases} \tag{10}$$

Step 4: Generation of the output voltage V_{ref}

The formula for determining output voltage (which should be achieved by modulation) V_{ref} depending on the standard vector of boundary voltages and the closing time of the key:

$$V_{ref} = \alpha V_1 + \beta V_2 \quad \text{where } \alpha = \frac{T_1}{T_S} \text{ and } \beta = \frac{T_2}{T_S} \tag{11}$$

Substitute Equation (10) into Equation (8):

$$V_{ref} = \sqrt{3}\left(\frac{V_{ref}}{V_{dc}}\right)\left[\sin\left(\theta - \frac{(k-1)\pi}{3}\right) + \sin\left(\frac{k\pi}{3} - \theta\right)\right] \tag{12}$$

Where the voltage modulation ratio can be expressed as:

$$V_{ref} = \sqrt{3}m\left[\sin\left(\theta - \frac{(k-1)\pi}{3}\right) + \sin\left(\frac{k\pi}{3} - \theta\right)\right] \tag{13}$$

And: $m = \frac{V_{ref}}{V_{dc}}$

This modulation offers very good performance and generates fewer current harmonics [5]. However, in practical implementation, the determination of the sequences does not involve a calculation of the tangent of the vector angle which causes undesirable singularities. This led us to consider DCSVM as the best duty cycle modulation technique for generating SVPWM signals. In the following, the DCSVM control strategy is applied to the structure shown in **Figure 2** and the results obtained from the simulation are discussed.

4. Results and Discussion

The simulation work is developed using Matlab/Simulink software in the case of a three-phase two-level voltage converter. The output signal of the DCSVM is then used to control the switch of the three-phase inverter and the parameters of simulation are giving to **Table 1**.

Using conventional SVM control, the control signals for the switches (S1, S2, S3, S4, S5, S6) are shown in **Figure 4**.

Table 1. The parameters and simulation conditions.

Parameters	Description	Values/Units
DC voltage source	V_{dc}	100 V
Internal resistance	R_{on}	1.8 mΩ
Snubber resistance	R_s	0.9 MΩ
Snubber capacitance	C_s	5 μF
Load resistance	$R_1 = R_2 = R_3$	20 Ω
Load inductance	$L_1 = L_2 = L_3$	20 mH
Modulation factor	m	0.9
Switching frequency	f	60 Hz
Carrier frequency	f_P	8 kHz
Half-carrier time period	T_s	0.5 ms

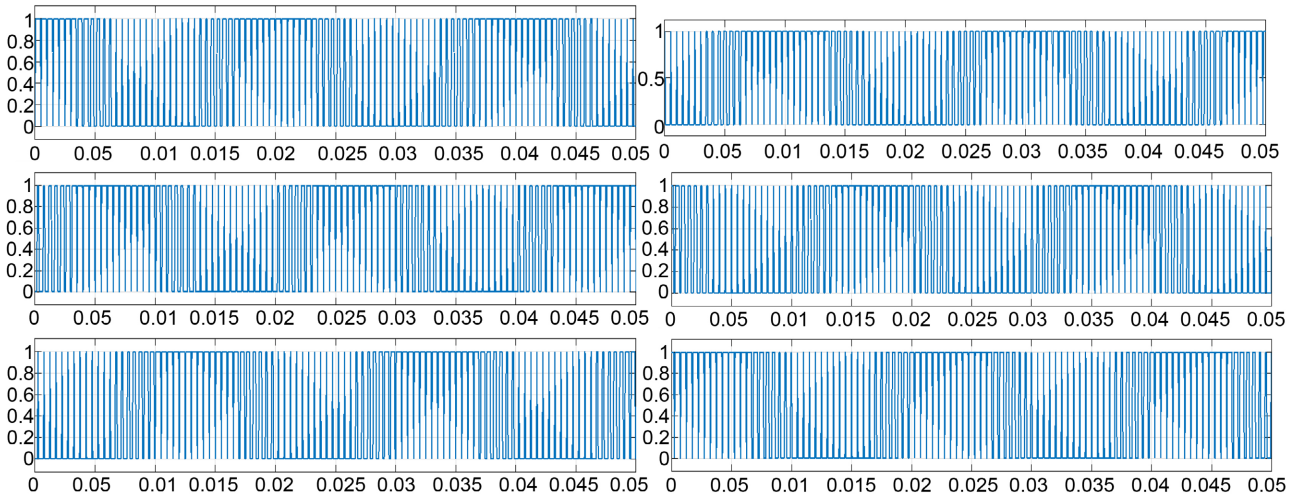

Figure 4. Control signals of the switches (S1, S2, S3, S4, S5, S6) with SVM control.

After the application of the DCSVM, we obtain the control signals of the switches (S1, S2, S3, S4, S5, S6) and the intermediate times (T_1, T_2, T_0) shown in Figure 5 and Figure 6.

Figure 7 shows the voltages (V_a, V_b, V_c) and currents (i_a, i_b, i_c) at the output of the inverter controlled by the SVM command.

The voltage and current signals in the load using the DCSVM control are shown in Figure 8 and Figure 9.

Figure 10 shows the voltage curve V_{ab} between phases a and b at the terminals of the inverter for the SVM and DCSVM controls.

The spectral analysis of the voltage and current signals using the Simulink POWERGUI FFT analysis tool with the SVM and DCSVM controls is shown in Figure 11 and Figure 12.

We note that the total harmonic distortion (THD) of the voltage and current give respectively 77.16% and 16.00%, with fundamental values of 47.27 V for the

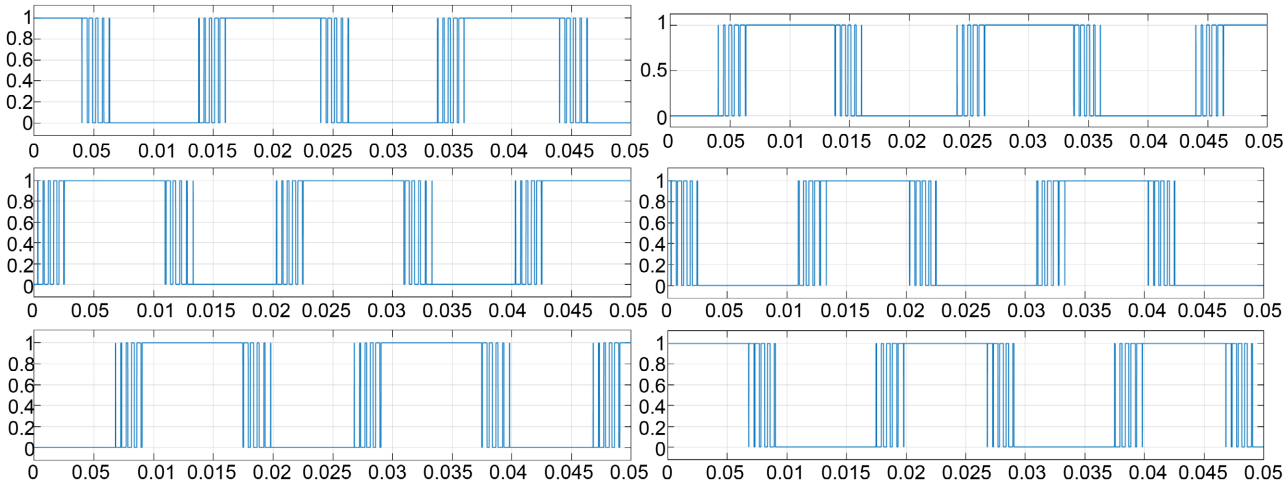

Figure 5. Switch control signals (S1, S2, S3, S4, S5, S6) with DCSVM control.

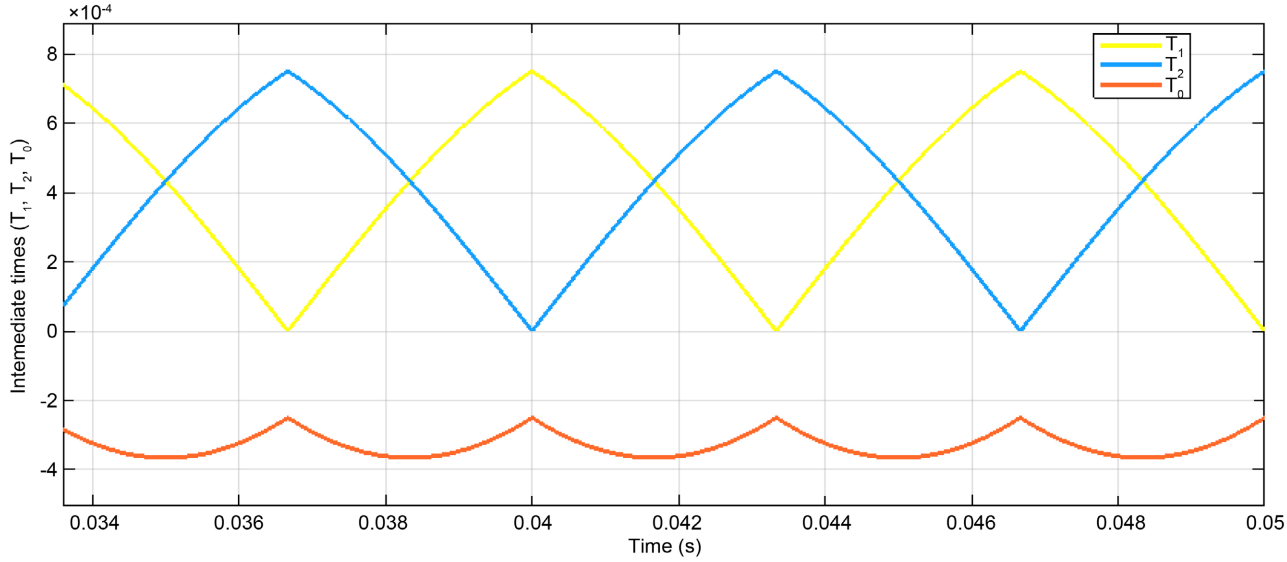

Figure 6. Intermediate times (T_1, T_2, T_0) with DCSVM control.

voltage and 2.01 A for the current in the case of the SVM control. The THDs of the voltage and current are too high compared to the limits set by the standard IEC 61000. **Figure 13** and **Figure 14** show the vectors generated by the SVM and DCSVM controls.

In **Figure 13(a)** and **Figure 14(a)**, the voltage vectors are the same in the case of SVM and DCSVM. In **Figure 13(b)**, the current vectors approach a circle with the SVM. On the other hand, the current vectors with the DCSVM give a hexagon (**Figure 14(b)**), expected that the DCSVM command is more precise than the SVM command. **Table 2** compares the results of the DCSVM with those of the SVM command.

After applying the DCSVM technique to the inverter of **Figure 2**, we obtain the total harmonic distortion (THD) of the voltage and the current give respectively 41.19% and 15.19% with fundamental values of 61.51 V for voltage and

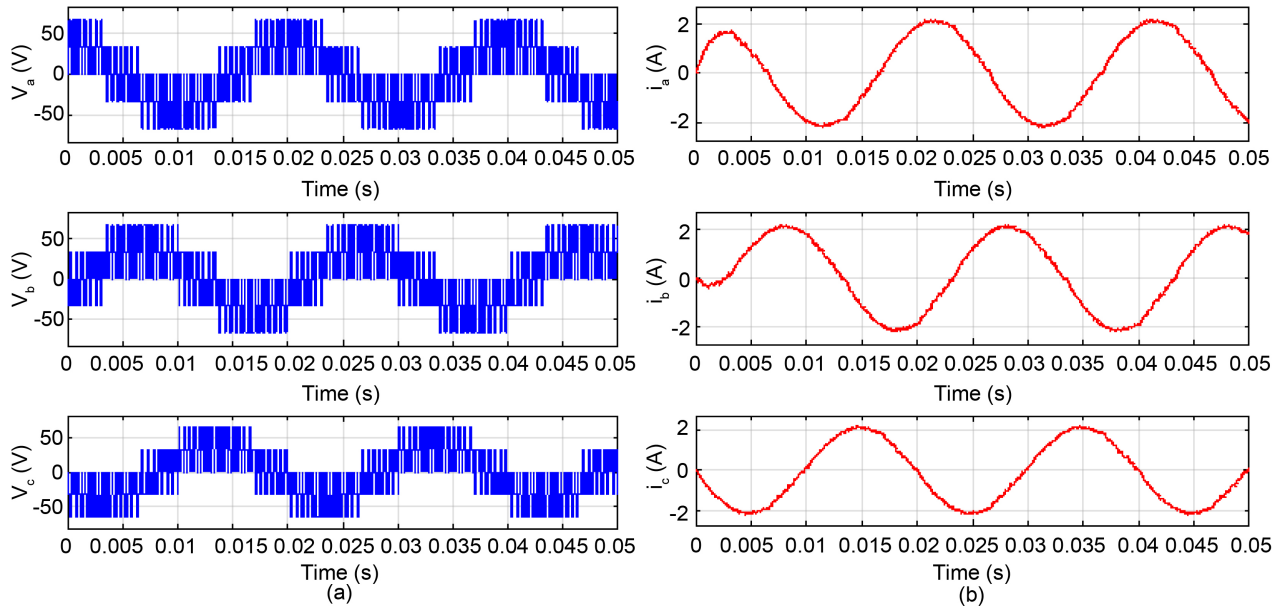

Figure 7. Voltages (V_a, V_b, V_c) and currents (i_a, i_b, i_c) with the SVM control.

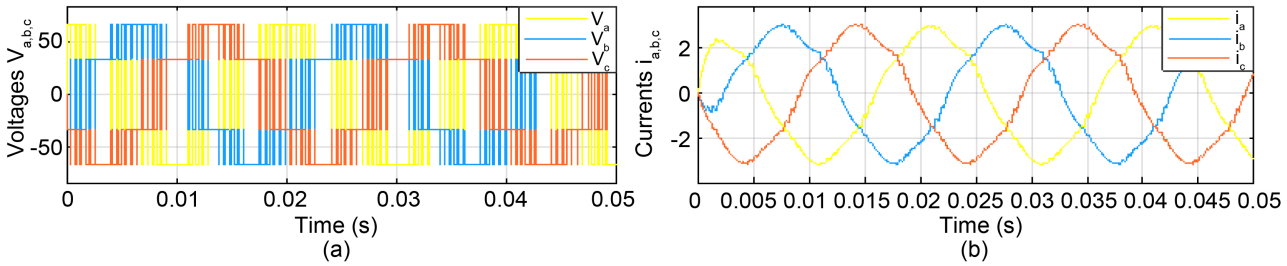

Figure 8. Voltages $V_{a,b,c}$ and currents $i_{a,b,c}$.

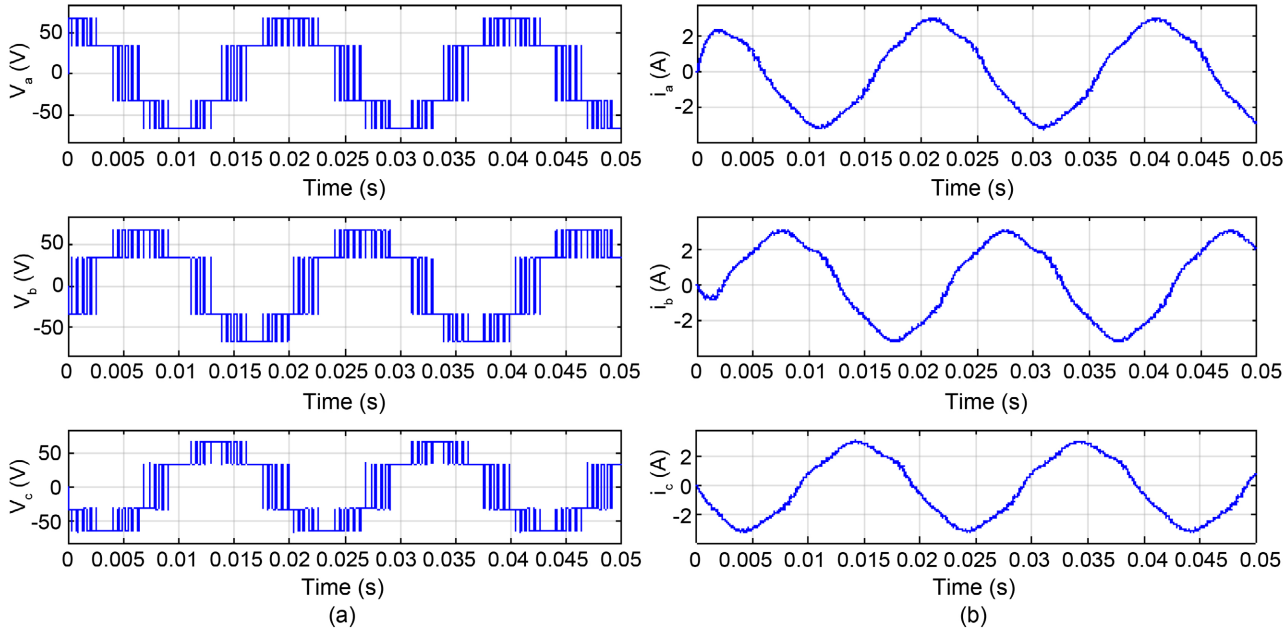

Figure 9. Voltages (V_a, V_b, V_c) and currents (i_a, i_b, i_c).

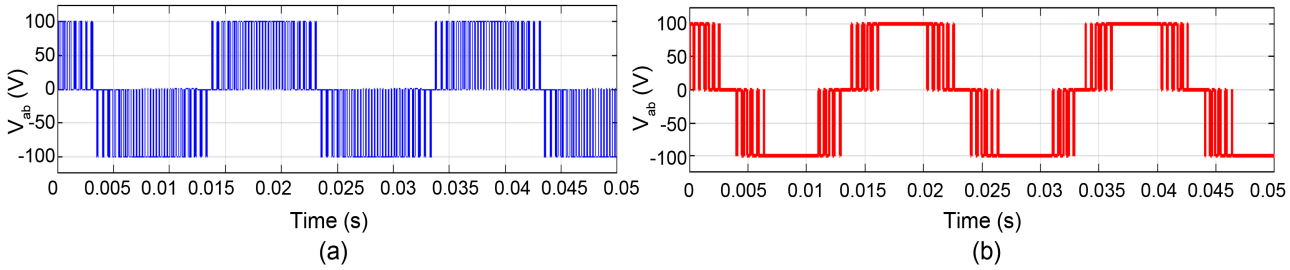

Figure 10. Voltage (V_{ab}): (a) with the SVM control and (b) with the DCSVM control.

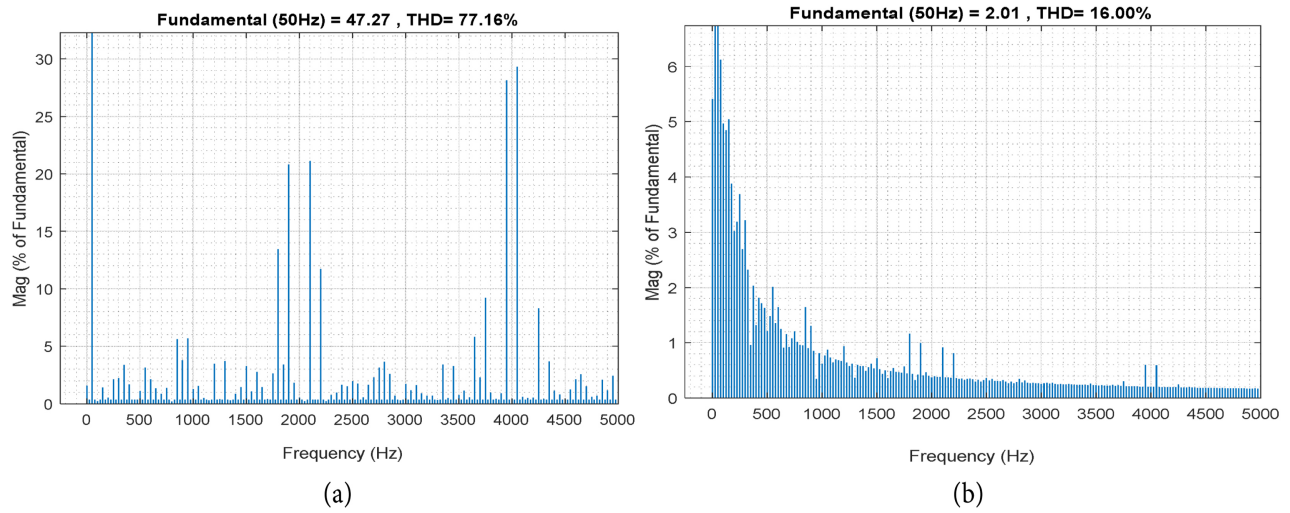

Figure 11. Harmonic spectrum of voltages (a) and currents (b) with the classical SVM.

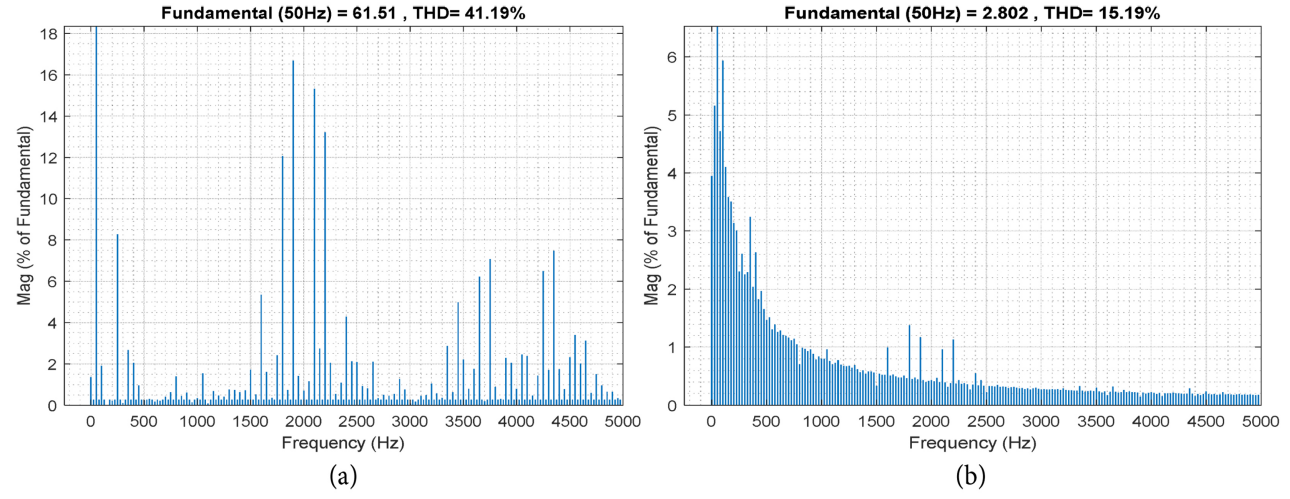

Figure 12. Harmonic spectrum of voltages (a) and currents (b) with the DCSVM.

2.80 A for current. Unlike DCSVM, SVM give 47.27 V for voltage and 2.01 A for current with THDs of 77.16% for voltage and 16.00% for current. This results in an improvement in the distortion rate of around 25.5%. These results show that the energy losses generated by the production of harmonics are recovered and materialized by the increase in voltage and current in the case of DCSVM.

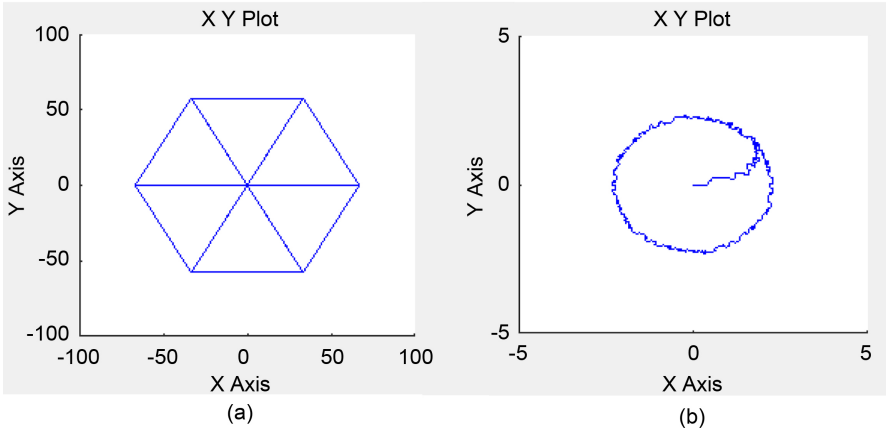

Figure 13. Output vectors of the three-phase inverter with the SVM control.

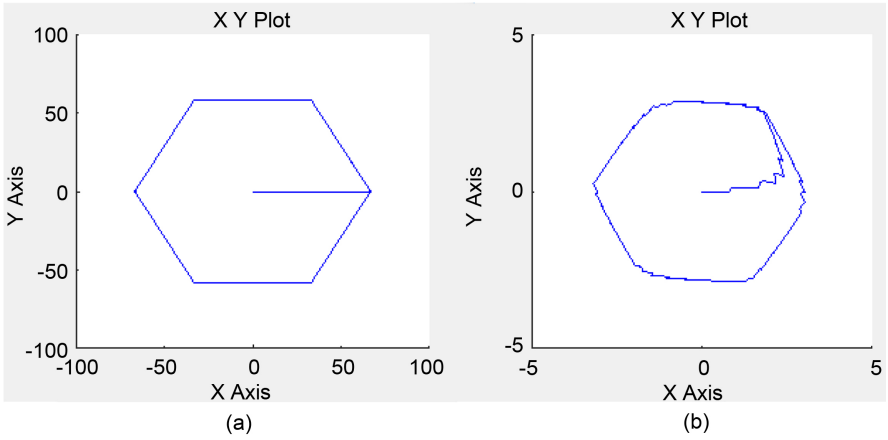

Figure 14. Output vectors of the three-phase inverter with the DCSVM control.

Table 2. Comparison of the results obtained at the output of the inverter.

Controls	THDV (%)	THDI (%)	Fundamentals	
			Voltage	Current
SVM	77.16	16.00	47.27	2.01
DCSVM	41.19	15.19	61.51	2.80

5. Conclusion

A new SVM control technique based on DCM has been developed using Matlab/Simulink software. We presented the principles of SVPWM and DCM followed by the description of the DCSVM (Duty Cycle Space Vector Modulation) strategy. Then, the structure of the DCSVM control and the implementation of a simulation model were presented. The simulation results obtained are better than those of the classical SVM control for similar simulation conditions. It is noted that the THDs of the voltage and current give 77.16% and 16.00% respectively, with fundamental values of 47.27 V for voltage and 2.01 A for current in the case of the SVM control. The THD of the voltage and current is too high compared to the limits set by the standard. The voltage vectors are the same in

the case of SVM and DCSVM and the current vectors approach a circle with SVM. On the other hand, the current vectors with the DCSVM give a hexagon, since the DCSVM control is more accurate than the SVM control. However, many studies can still be conducted and we suggest an experimental verification of the proposed approach.

Conflicts of Interest

The authors declare no conflicts of interest regarding the publication of this paper.

References

[1] Adamou, M., Alkassoum, N., Foulani, A. and Maiga, A.S. (2020) Clean-Up of Electrical Grid Harmonic: A Comparative Study of the Control of Three-Phase Shunts Active Filters, by Pulse Width Modulation and by Hysteresis. *International Journal of Innovation and Applied Studies*, **28**, 557-566.

[2] Biyobo, A.O., Nneme, L.N., Mbihi, J., Pauné, F. and Moffo, B.L. (2020) Experimental Study of a New Model of Single-Phase Solar Inverter with Duty Cycle Modulation. *Africa Science*, **16**, 118.

[3] Pesdjock, M.J.P., Mboupda Pone, J.R., Tchiotsop, D., Douanla, M.R. and Kenne, G. (2021) Minimization of Currents Harmonics Injected for Grid Connected Photovoltaic Systems Using Duty-Cycle Modulation Technique. *International Journal of Dynamics and Control*, **9**, 1013-1023. https://doi.org/10.1007/s40435-020-00718-8

[4] Podder, A.K., Habibullah, M., Tariquzzaman, M., Hossain, E. and Padmanaban, S. (2020) Power Loss Analysis of Solar Photovoltaic Integrated Model Predictive Control Based on Grid Inverter. *Energies*, **13**, 4669. https://doi.org/10.3390/en13184669

[5] Bouyakoub, I., Taleb, R., Mellah, H. and Zerglaine, A. (2020) Implementation of Space Vector Modulation for Two Level Three-Phase Inverter Using dSPACE DS1104. https://doi.org/10.2139/ssrn.3918716

[6] Zhang, G., Wan, Y., Wang, Z., Gao, L., Zhou, Z. and Geng, Q. (2020) Discontinuous Space Vector PWM Strategy for Three-Phase Three-Level Electric Vehicle Traction Inverter Fed Two-Phase Load. *World Electric Vehicle Journal*, **11**, Article No. 27. https://doi.org/10.3390/wevj11010027

[7] Nguefack, L.T., Kenfack, G.W. and Mbihi, J. (2020) A Novel Optical Fiber Transmission System Using Duty-Cycle Modulation and Application to ECG Signal: Analog Design and Simulation. *Journal of Electrical Engineering, Electronics, Control and Computer Science*, **6**, 39-48.

[8] Yang, Y., Qin, Y., Tan, S.C. and Hui, S.Y.R. (2020) Reducing Distribution Power Loss of Islanded AC Microgrids Using Distributed Electric Springs with Predictive Control. *IEEE Transactions on Industrial Electronics*, **67**, 9001-9011. https://doi.org/10.1109/TIE.2020.2972450

[9] Joseph, K.K., Léandre, N.N. and Salomé, N.E. (2020) Contribution to the Optimization of the Transient Stability of an Electric Power Transmission Network Using a Universal Power Flow Compensator Controlled by a Three-Stage Inverter. *World Journal of Engineering and Technology*, **8**, 675-688. https://doi.org/10.4236/wjet.2020.84048

[10] Dadjé, A., Djongyang, N. and Tchinda, R. (2017) Electrical Power Losses in a Photovoltaic Solar Cell Operating under Partial Shading Conditions. *Journal of Power and Energy Engineering*, **5**, 19. https://doi.org/10.4236/jpee.2017.510002

[11] Ngaleu, G.M., Kom, C.H., Yeremou, A.T., Eke, S. and Nanfak, A. (2021) Design of New Duty-Cycle Modulator Structures for Industrials Applications, an Alternative to Pulse-Width Modulation. *European Journal of Electrical Engineering*, **23**, 103-111. https://doi.org/10.18280/ejee.230203

[12] Biyobo, A.O., Nneme, L.N. and Mbihi, J.E.A.N. (2018) A Novel Sine Duty Cycle Modulation Control Scheme for Photovoltaic Single Phase Power Inverters. *WSEAS Transactions on circuits and Systems*, **17**, 107-113.

[13] Sonfack, G., Mbihi, J. and Moffo, B.L. (2018) Optimal Duty-Cycle Modulation Scheme for Analog-to-Digital Conversion Systems. *International Journal of Electronics and Communication Engineering*, **11**, 354-360.

[14] Mbihi, J., Ndjali, B. and Mbouenda, M. (2005) Modelling and Simulation of a Class of Duty-Cycle Modulators for Industrial Instrumentation. *Iranian Journal of Electrical and Computer Engineering*, **4**, 121-128.

[15] Moffo, B.L., Mbihi, J. and Nneme, L.N. (2014) A Low Cost and High Quality Duty-Cycle Modulation Scheme and Applications. *International Journal of Electrical*, *Computer*, *Energetic*, *Electronic and communication Engineering*, **8**, 82-88.

[16] Nnem, L.N., Lonla, B.M. and Mbihi, J. (2018) Review of a Multipurpose Duty-Cycle Modulation Technology in Electrical and electronics engineering. *Journal of Electrical Engineering*, *Electronics*, *Control and Computer Science*, **4**, 9-18.

[17] Mbihi, J., Beng, F.N., Kom, M. and Nneme, L.N. (2012) A Novel Analog-to-Digital Conversion Technique Using Nonlinear Duty-Cycle Modulation. *International Journal of Electronics and Computer Science Engineering*, **1**, 818-825.

[18] Mbihi, J. (2017) Dynamic Modelling and Virtual Simulation of Digital Duty-Cycle Modulation Control Drivers. *International Journal of Electrical*, *Computer*, *Energetic*, *Electronic and Communication Engineering*, **11**, 472-477.

[19] Agu, M.U., Ejiogu, E.C., Nnadi, D.B.N. and Eya, C.U. (2021) A Grid Tied Short-Through Proof Solar PV Inverter. *IOP Conference Series*: *Earth and Environmental Science*, **730**, Article ID: 012017. https://doi.org/10.1088/1755-1315/730/1/012017

[20] Jiang, W., Wang, P., Ma, M., Wang, J., Li, J., Li, L. and Chen, K. (2019) A Novel Virtual Space Vector Modulation with Reduced Common-Mode Voltage and Eliminated Neutral Point Voltage Oscillation for Neutral Point Clamped Three-Level Inverter. *IEEE Transactions on Industrial Electronics*, **67**, 884-894. https://doi.org/10.1109/TIE.2019.2899564

[21] Alqarni, Z. and Asumadu, J.A. (2020) A Synchronized Grid Integrated Three-Phase Inverter with a Renewable Source for Power Sharing. *Journal of Power and Energy Engineering*, **8**, 88-101. https://doi.org/10.4236/jpee.2020.83006

[22] Ramasamy, P. and Krishnasamy, V. (2020) SVPWM Control Strategy for a Three Phase Five Level Dual Inverter Fed Open-End Winding Induction Motor. *ISA Transactions*, **102**, 105-116. https://doi.org/10.1016/j.isatra.2020.02.034

[23] Bonkoungou, D., Korsaga, É., Guingané, T., Tassembédo, S., Koalaga, Z. and Zougmoré, F. (2022) Study and Design of a DC/AC Energy Converter for PV System Connected to the Grid Using Harmonic Selected Eliminated (HSE) Approach. *Open Journal of Applied Sciences*, **12**, 301-316. https://doi.org/10.4236/ojapps.2022.123022

[24] Dandoussou, A., Kenfack, P., Perabi, S.N. and Kamta, M. (2021) Simulations of the Performance of Maximum Power Point Tracking Algorithms Based on Experimental Data According to the Topologies of DC-DC Converters. *Journal of Power and Energy Engineering*, **9**, 76-92. https://doi.org/10.4236/jpee.2021.95005

[25] Periyanayagam, M., Kumar, V.S., Chokkalingam, B., Padmanaban, S., Mihet-Popa, L. and Adedayo, Y. (2020) A Modified High Voltage Gain Quasi-Impedance Source Coupled Inductor Multilevel Inverter for Photovoltaic Application. *Energies*, **13**, Article No. 874. https://doi.org/10.3390/en13040874

[26] Nneme, L.N. and Mbihi, J. (2014) Modeling and Simulation of a New Duty-Cycle Modulation Scheme for Signal Transmission Systems. *American Journal of Electrical and Electronic Engineering*, **2**, 82-87. https://doi.org/10.12691/ajeee-2-3-4

[27] Sun, J. (2012) Pulse-Width Modulation. In: Vasca, F. and Iannelli, L., Eds., *Dynamics and Control of Switched Electronic Systems*, Springer, London, 25-61. https://doi.org/10.1007/978-1-4471-2885-4_2

[28] Louossi, T., Djongyang, N., Mayi, O.T.S. and Nanfak, A. (2020) Perturb and Observe Maximum Power Point Tracking Method for Photovoltaic Systems Using Duty-Cycle Modulation. *Journal of Renewable Energies*, **23**, 159-175.

[29] Moffo, B.L., Mbihi, J., Nneme, L.N. and Kom, M. (2013) A Novel Digital-to-Analog Conversion Technique Using Duty-Cycle Modulation. *International Journal of Circuits*, *Systems and Signal Processing*, **7**, 42-49.

[30] Mbihi, J. and Nneme, L.N. (2013) A Novel Control Scheme for Buck Power Converters Using Duty-Cycle Modulation. *International Journal of Power Electronics*, **5**, 185-199. https://doi.org/10.1504/IJPELEC.2013.057038

[31] Paulin, D., Jean, M., Djalo, H. and Joseph, E. (2017) Virtual Digital Control Scheme for a Duty-Cycle Modulation Boost Converter. *Journal of Computer Science and Control Systems*, **10**, 22-27.

[32] Nna, T.P.N., Essiane, S.N. and Ngoffé, S.P. (2020) Control of an Active Filter by Duty Cycle Modulation (DCM) for the Harmonic Decontamination of a Three-Phase Electrical Network. *Journal of Power and Energy Engineering*, **8**, 1-14. https://doi.org/10.4236/jpee.2020.87001